JOURNAL OF MORPHOLOGY 207:327–344 (1991)

The Functional Anatomy of the Shoulder in the European Starling (*Sturnus vulgaris*)

KENNETH P. DIAL, G.E. GOSLOW, JR.,
AND FARISH A. JENKINS, JR.
Museum of Comparative Zoology, Harvard University, Cambridge, Massachusetts 02138

ABSTRACT The excursions of wing elements and the activity of eleven shoulder muscles were studied by cineradiography and electromyography in European starlings (*Sturnus vulgaris*) flying in a wind tunnel at speeds of 9–20 m s^{-1}.

At the beginning of downstroke the humerus is elevated 80–90° above horizontal, and both elbow and wrist are extended to 90° or less. During downstroke, protraction of the humerus (55°) remains constant; elbow and wrist are maximally extended (120° and 160°, respectively) as the humerus passes through a horizontal orientation. During the downstroke-upstroke transition humeral depression ceases (at about 20° below horizontal) and the humerus begins to retract. However, depression of the distal wing continues by rotation of the humerus and adduction of the carpometacarpus. Humeral retraction (to within about 30° of the body axis) is completed early in upstroke, accompanied by flexion of the elbow and carpometacarpus. Thereafter the humerus begins to protract as elevation continues. At mid-upstroke a rapid counterrotation of the humerus reorients the ventral surface of the wing to face laterad; extension of the elbow and carpometacarpus are initiated sequentially. The upstroke-downstroke transition is characterized by further extension of the elbow and carpometacarpus, and the completion of humeral protraction.

Patterns of electromyographic activity primarily coincide with the transitional phases of the wingbeat cycle rather than being confined to downstroke or upstroke. Thus, the major downstroke muscles (pectoralis, coracobrachialis caudalis, sternocoracoideus, subscapularis, and humerotriceps) are activated in late upstroke to decelerate, extend, and reaccelerate the wing for the subsequent downstroke; electromyographic activity ends well before the downstroke is completed. Similarly, the upstroke muscles (supracoracoideus, deltoideus major) are activated in late downstroke to decelerate and then reaccelerate the wing into the upstroke; these muscles are deactivated by mid-upstroke. Only two muscles (scapulohumeralis caudalis, scapulotriceps) exhibit electromyographic activity exclusively during the downstroke. Starlings exhibit a functional partitioning of the two heads of the triceps (the humerotriceps acts with the pectoralis group, and does not overlap with the scapulotriceps). The biphasic pattern of the biceps brachii appears to correspond to this partitioning.

Current understanding of the wing mechanics of birds has been based primarily on external observations and measurements (Brown, '48, '63; Simpson, '83; Rayner, '79a,b). Up to the present, electromyographic studies of birds have focused almost exclusively on the pectoralis muscle (Hagiwara et al., '68; Aulie, '70; Goldspink et al., '78; Dial et al., '87, '88). Recently, we reported on a cineradiographic analysis of the starling shoulder (Jenkins et al., '88). We present

Kenneth P. Dial is now at the Division of Biological Sciences, University of Montana, Missoula, MT 59812. G.E. Goslow, Jr., is now at the Section for Population Biology, Morphology and Genetics, Brown University, Providence, RI 02912.
Authors listed alphabetically.

here the results from an analysis of patterns of muscle activity and movements of the wing skeleton through the combined use of electromyography, cineradiography, and cinematography of European starlings (*Sturnus vulgaris*) flying in a wind tunnel. This study was undertaken to provide a more comprehensive account of the function of the wing's musculoskeletal system in flight, and to compare avian data with that known from other flying and terrestrial vertebrates.

MATERIALS AND METHODS

Wind tunnel

A 5-m-long, variable-speed wind tunnel was assembled from four individual sections (fan, transition, 56 × 56 × 88 cm plexiglass flight chamber, and intake funnel). The fan (blade diameter 81 cm) was powered with a 20-hp DC motor supplied with 16 deep cycle 6-volt batteries connected in series to produce 96 volts. Airspeed was controlled with a dashpot rheostat and wind velocities were read from an airspeed indicator connected to a pitot tube located within the tunnel. Laminar air flow was developed by a 10-cm-thick portion of aluminum honeycomb (cell diameter 3.2 mm) located between the intake section and flight chamber.

Animals and flight training

The 26 adult European starlings (*Sturnus vulgaris*) used in this study were captured from wild populations in Arizona and Massachusetts. Six starlings were dissected for anatomical study, four were used for cineradiographic analysis, and sixteen were surgically implanted with fine wires for electromyographic experiments. Animals were housed in two stainless steel wire mesh cages (1.3 m × 1 m × 1 m) and were maintained with water (*ad libitum*), fruit, canned dog food, vitamin supplements, and mealworms.

Starlings were introduced into the flight chamber at wind velocities between 25 and 35 mph (10–16 m s^{-1}). Flight conditioning continued twice a day until individuals maintained steady flight for 5 minutes or more. On average only one of five birds captured was suitable for experiments, a success rate similar to that of Torre-Bueno and Larochelle ('78).

Cineradiography and cinematography

Siemens cineradiographic apparatus (grid-controlled tube with a 0.06-mm focal spot, 27.94-cm Sirecon image intensification system), coupled with an Eclair GV16 high-speed 16-mm cine camera operated at 200 frames s^{-1}, was positioned for lateral or dorsoventral projections.

The four starlings used for the x-ray analyses were surgically implanted with carbide steel pin markers (ca. 0.5 mm wide, 2.5 mm long) under deep anaesthesia (ketamine, 25 mg/kg; xylazine, 2 mg/kg I.M.). Markers were placed in the anterior and posterior ends of the sternal carina, both acrocoracoids, and the deltopectoral crest of one humerus. Other skeletal features (e.g., coracosternal joint, bones of the antebrachium and carpometacarpus) were readily visualized without markers. A 10-mm wire, 0.9 mm in diameter, was inserted subcutaneously above the vertebral column as a scale and reference point for film analysis.

From approximately 5,000 feet of Kodak Plus-X Reversal film, flight sequences were selected that provided good resolution of the complete wing skeleton during consecutive wingbeats. These sequences were analyzed frame by frame with a Vanguard M-C11P film analyzer coupled with a Graf/Pen Sonic digitizer and IBM-AT and Apple II computers. The position of shoulder and wing elements was plotted frame by frame for approximately 100 wingbeat cycles from both dorsoventral and lateral projections. Skeletons of two adult birds, mounted to duplicate the perceived angles recorded cineradiographically, were used to estimate the actual positional relations of wing elements.

Approximately 1,000 feet of light film (Kodak Color, 3200K Tungsten) was taken of two birds with a Photosonics 16-1PL camera at 500 frames s^{-1}. An electrical spike emitted from the camera synchronized each frame of film with the electromyographic record.

Electromyography

Sixteen birds were anaesthetized (as above) and surgically implanted with chronic bipolar electrodes (insulated silver, 100 μm diameter, 0.5-mm tip exposure, 0.5-mm intertip distance) with the aid of a 23-gauge hypodermic needle. A skin incision and blunt dissection exposed each muscle for positive identification. Electrodes were sutured to adjacent periosteum or fascia, and led subcutaneously to a 12-pole miniature connector (Microtech) fixed on the bird's back. Electrode positions were verified by post-mortem dissection.

Birds were conditioned to flight in the wind tunnel prior to implant surgery. Recordings were made during the first and second postop-

erative days. Simultaneous electromyograms (EMGs) were recorded from a maximum of five muscles. The pectoralis was used as a reference muscle in all experiments. Each signal was amplified × 50–2,000 (Grass P511) and recorded on tape at 38.1 cm s^{-1} (Bell and Howell CPR 4010 FM tape recorder). Recordings were played at 4.76 cm s^{-1} (one-eighth of the recorded speed) into a chart recorder (Gould Brush Model 240) after being filtered (100 Hz high band pass; 30,000 Hz low band pass). Fast-Fourier Transform analyses of raw EMGs revealed that the power spectrum of these signals is between 100 and 2,000 Hz.

EMGs recorded from sequences of steady flight were processed by a Keithley DAS Series 500 analog-to-digital (A/D) converter at a sampling rate of 2,150 Hz per channel; signals played back at one-fourth the original speed resulted in an effective sampling rate of 8,600 Hz and were stored on disk (IBM-AT computer). Digital data were then visually inspected by sending the stored data through the A/D converter to a Tektronix 4208 Graphics Terminal. We employed computer software developed by G.V. Lauder (see Bemis and Lauder, '86; Shaffer and Lauder, '85) to analyze the onset and offset times of muscles relative to that of the pectoralis pars sternobrachialis (selected as a reference muscle). Mean onset and offset times and Standard Errors were calculated for each muscle from 20 wingbeat cycles (10 cycles each from two birds), with the exception of the subscapularis (10 cycles only).

RESULTS

Myology

The nomenclature follows Vanden Berge ('79).

M. biceps brachii (Figs. 1, 2, 5)

The muscle originates primarily by a stout tendon from the lateral aspect of the acrocoracoid process (Fig. 5). In crossing the shoulder joint the tendon spreads into a broad aponeurosis that is attached to the cranial (i.e., flexor) surface of the Crista bicipitalis of the humerus, thus forming a second origin (Fig. 2). The muscle inserts on both the ulna

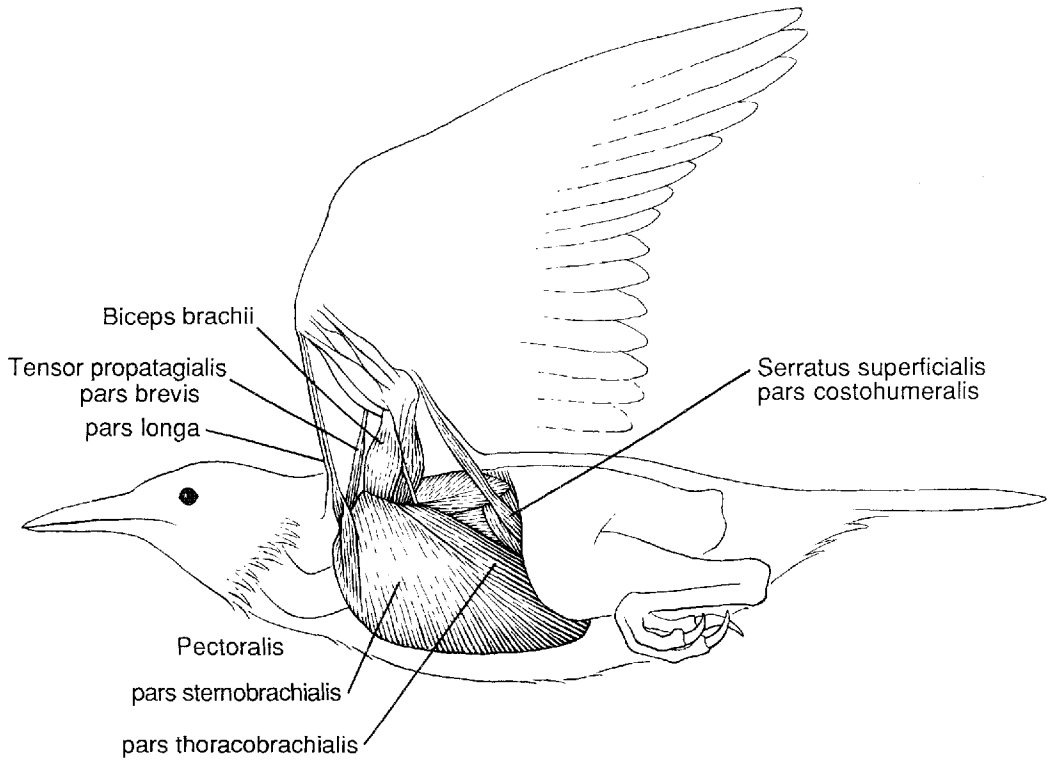

Fig. 1. Lateral view of the superficial muscles of the shoulder in the European starling (*Sturnus vulgaris*).

and the radius. The ulnar insertion is by a tendon that passes into a fossa on the flexor surface of the proximal ulna. The radial tendon is only about one-tenth the diameter of the ulnar, and attaches to the bicipital tubercle.

M. coracobrachialis caudalis (Figs. 2,4,5)

The muscle takes origin from the caudal aspect of the ventral two-thirds of the coracoid (including the lateral aspect of the lateral process), as well as by fibers that arise directly from fascia overlying the lateral aspect of the sternocoracoideus (Fig. 2). The insertion is into the distal part of the Tuberculum ventrale between the two pneumotricipital fossae (Fig. 4).

M. deltoideus major pars caudalis (Fig. 3)

The larger of the two deltoid heads arises from the medial aspect of the acrocoracoid and the adjacent dorsal process of the furcula (Extremitas omalis claviculae or Epicleideum). An accessory slip originates as a slender tendon from the cranial margin of the Foramen triosseum, adjacent to the origin of the M. deltoideus minor. The muscle is wrapped around a sesamoid, the Os humerocapsularis, on the dorsal aspect of the humeral head which serves as the origin of the cranial deltoid. The traction of the fibers is thus redirected from a posterior to a posterolateral direction. The muscle inserts on the dorsal humeral epicondyle.

M. deltoideus major pars cranialis (Figs. 3,4)

The smaller of the two major deltoid heads is attached proximally to the Os humerocapsularis. This sesamoid lies on the dorsal side of the humeral head, to which it is attached by a ligament; the ligament is perforated by the tendon of the supracoracoideus and thus also serves as a trochlea (Fig. 3). The humerocapsular bone is also firmly attached to the

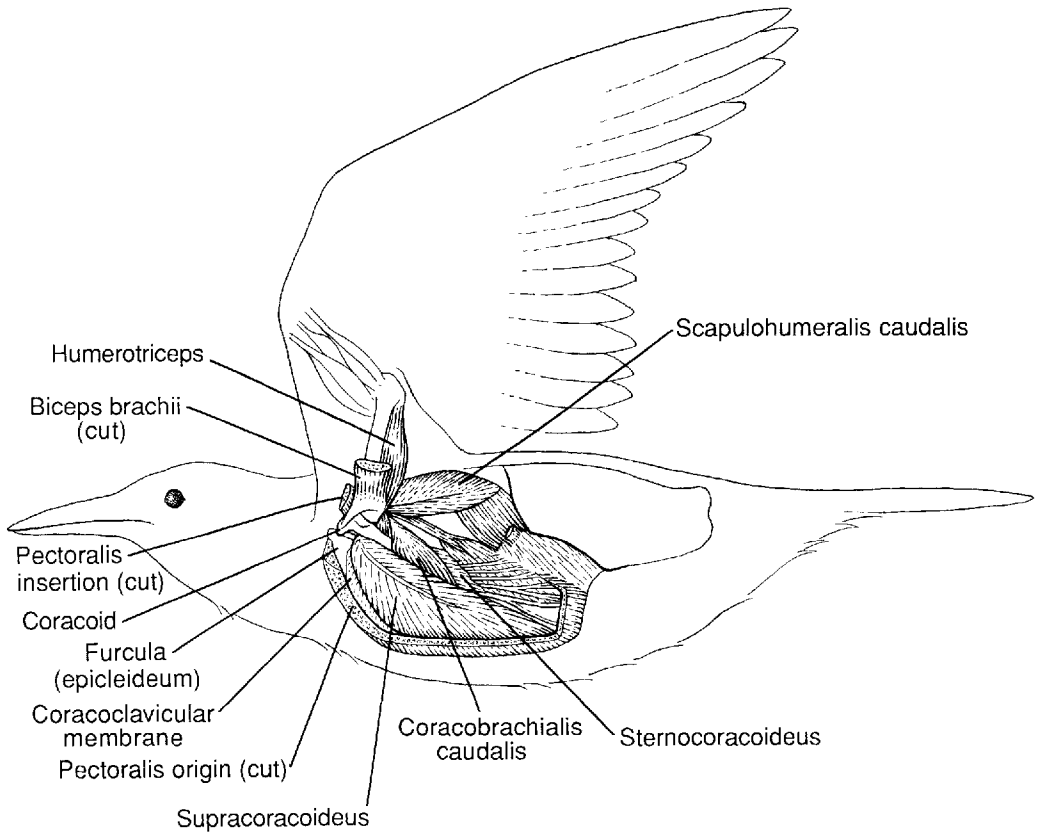

Fig. 2. Lateral view of some of the deep muscles of the shoulder in the European starling (*Sturnus vulgaris*); the pectoralis major has been resected, leaving only its origin and insertion.

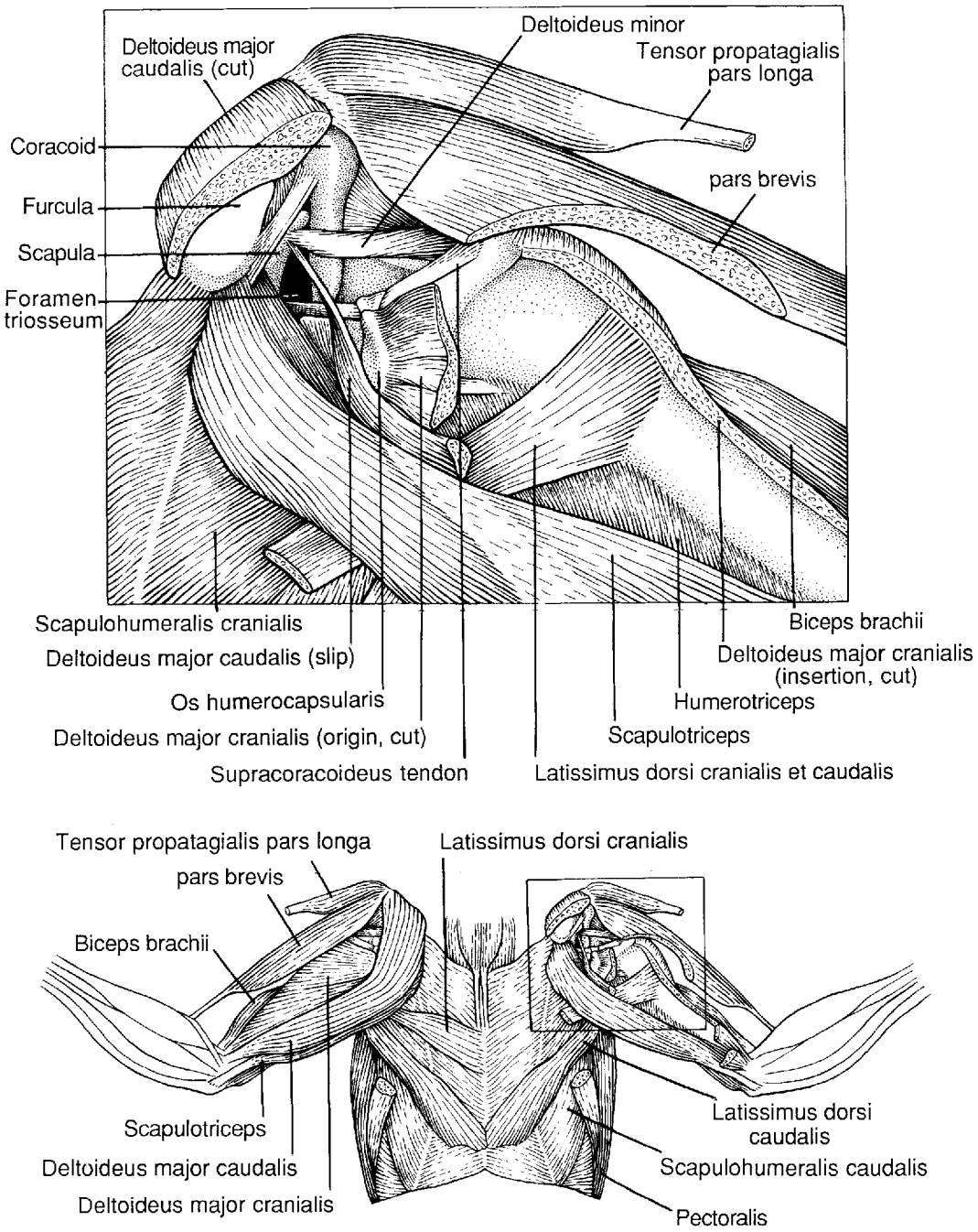

Fig. 3. Dorsal view of the shoulder muscles in the European starling (*Sturnus vulgaris*). **Below:** on the left side the superficial muscles of the shoulder are shown intact; on the right side parts of the latissimus dorsi caudalis, deltoideus major cranialis et caudalis, and tensor propatagialis pars brevis have been resected to display deeper structures. Details of structures within the inset are shown above.

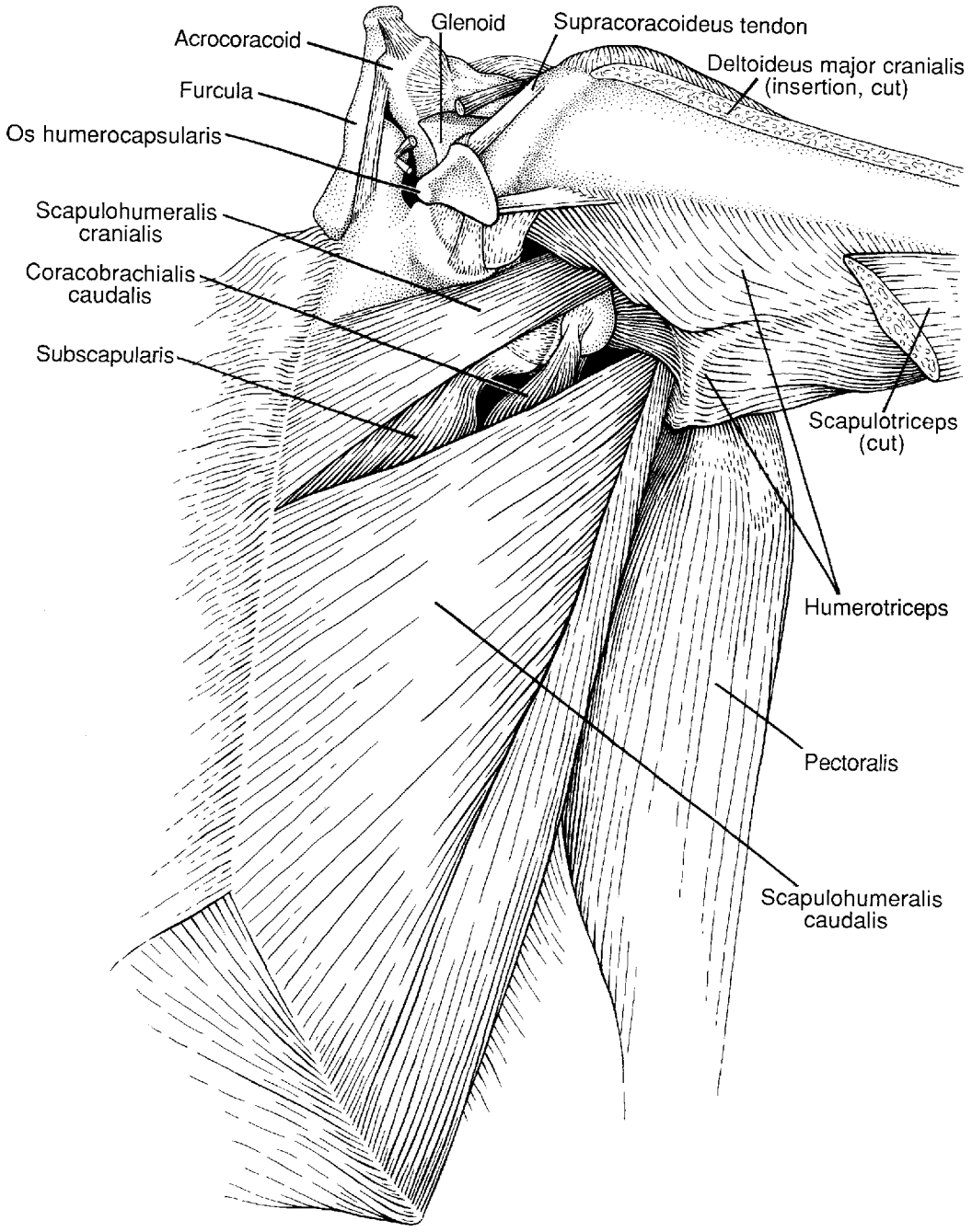

Fig. 4. Dorsal view of the right shoulder joint in the European starling (*Sturnus vulgaris*). Superficial muscles, including the latissimus dorsi cranialis et caudalis, deltoideus major cranialis et caudalis, and tensor propatagialis pars longa et pars brevis, have been completely removed.

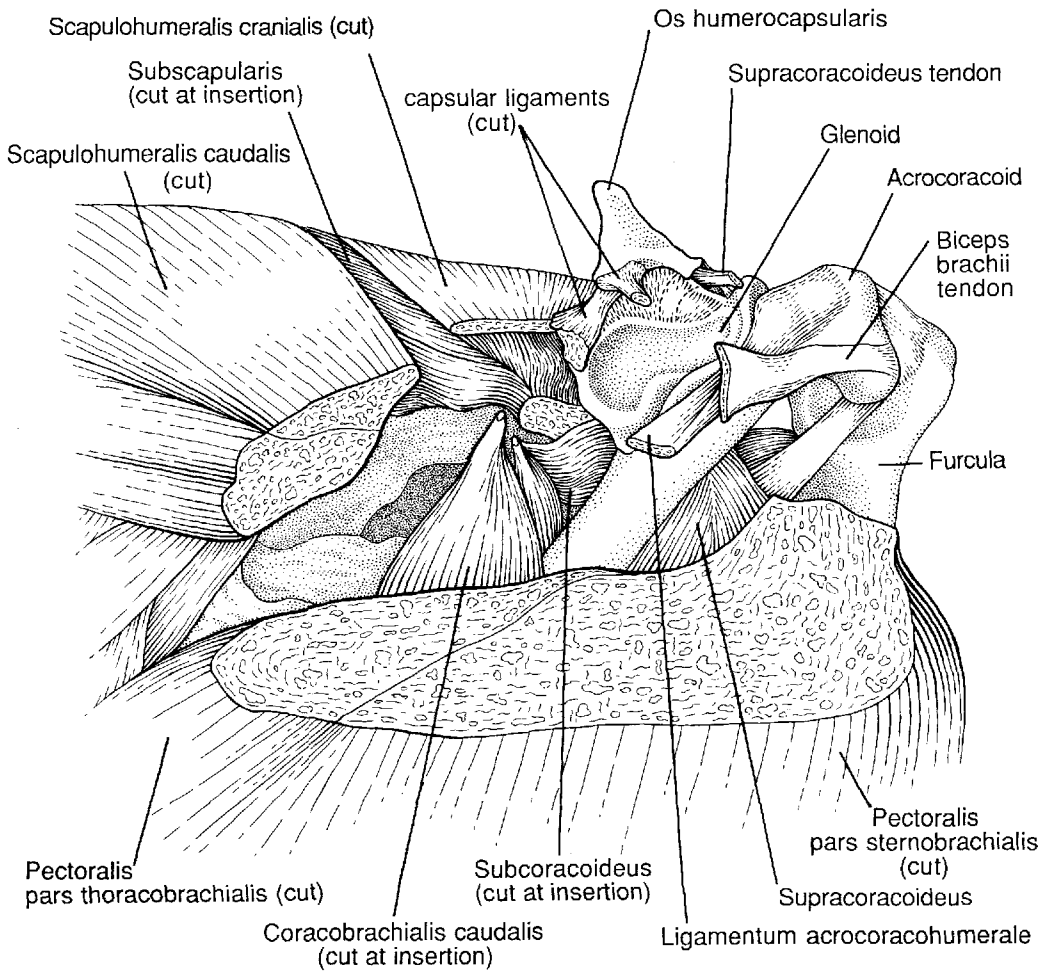

Fig. 5. Lateral view of the right shoulder in the European starling (*Sturnus vulgaris*). The humerus has been removed, and the pectoralis and scapulohumeralis caudalis resected, to show the musculotendinous and ligamentous structures that intimately surround the joint.

capsule of the glenohumeral joint, and by ligaments (represented by thickened part of the capsule) to the dorsocaudal margin of the glenoid (Fig. 5). The broad insertion of the cranial head of the deltoid begins on the dorsal surface of the deltopectoral crest, continues along the anterior aspect of the humeral shaft, and ends in a tendon inserted into the dorsal epicondyle.

M. pectoralis (Figs. 1–5)

As in many birds, the pectoralis is composed of two parts partially separated by an intramuscular tendon. The cranial part, pars sternobrachialis (SB), arises along the entire furcular shaft from a region inferior to the coracoclavicular articulation to the furcular apophysis (or Hypocleideum), and from the membrane joining the Hypocleideum and sternum. Additional fibers arise from the coracoclavicular membrane. The remainder of the SB takes origin along the ventral one-third of the lateral aspect of the carina including its entire margin. The caudal part of the pectoralis, pars thoracobrachialis (TB), arises from the caudal margin of the lateral plate of the sternum, from the membrane of the lateral notch, and from the lateral trabecula; the fibers along the superocaudal border of the muscle attach to the external abdominal oblique muscle. The pectoralis insertion onto the deltopectoral crest is musculotendinous;

the muscular fibers are derived from the SB, and lie dorsad to the intramuscular tendon. Within the muscle belly the intramuscular tendon is a broad sheet that receives the insertion of the SB fibers on its dorsolateral aspect and TB fibers on its ventromedial aspect.

M. scapulohumeralis caudalis (Figs. 2–5)

The muscle originates from the caudal two-thirds of the scapula. Anterior fibers arise primarily from the medial aspect of the scapula, whereas posterior fibers arise from the lateral margin and ventral aspect of the blade. The insertion is by a tendon into the dorsal surface of the proximal humerus. The tendon passes between two heads of the humeral triceps, and inserts into the caudal (distal) pneumotricipital fossa. In crossing the shoulder joint, the muscle lies lateral to the coracobrachialis caudalis (Fig. 4).

M. sternocoracoideus (Fig. 2)

The sternocoracoideus arises from the anterior margin and lateral aspect of the craniolateral process of the sternum. The relatively short muscle fibers pass anteromedially to insert on the ventral half of the coracoid; the insertion area extends from the posterior margin of the lateral process along the medial side of the coracoid to its midpoint.

M. subscapularis (Figs. 4,5)

The muscle arises by two heads from the anterior third of the scapular blade. The origin of the lateral head extends from the caudal margin of the glenoid along the lateral margin and ventral surface of the scapula. The medial head arises entirely from the ventral scapular surface. The anterolaterally directed fibers converge on a short tendon to insert into the Tuberculum ventrale on the proximal humerus. The two heads are separated by the insertion of the M. serratus superficialis onto the scapula.

M. supracoracoideus (Figs. 2–5)

The origin of the bipinnate supracoracoideus extends from the ventral part of the coracoclavicular membrane cranially almost to the caudal end of the sternum (Fig. 2). A few fibers arise from the coracoid adjacent to the coracosternal joint. The majority attach along the surface of the lateral plate of the sternum (excluding the lateral trabecula and membrane of the lateral notch) as well as on the dorsal two-thirds of the lateral aspect of the carina. The tendon of the supracoracoideus traverses the Foramen triosseum and then passes anterolaterally to insert into a tuberosity on the dorsal aspect of the humeral head (Figs. 3,4) that lies between two pneumatic foramina.

M. humerotriceps (Figs. 3,4)

The muscle arises by two heads from the pneumotricipital fossae and their margins on the proximal, dorsal surface of the humerus. Most fibers converge on a central tendon that is inserted into the olecranon process of the ulna; some attach directly to the olecranon.

M. scapulotriceps (Figs. 3,4)

The scapulotriceps arises from the medial surface and dorsal margin of the Epicleideum, and to a lesser extent from a dense band of connective tissue joining the apices of the coracoid and furcula. The muscle passes caudodorsally over the shoulder joint and inserts on the olecranon process of the ulna. A sesamoid is lodged in the tendon as it crosses the elbow.

Kinematics

The wingbeat cycle may be divided for descriptive purposes into four phases: downstroke, downstroke-upstroke transition, upstroke, and upstroke-downstroke transition. Downstroke and upstroke are defined by humeral depression and elevation, respectively. The downstroke typically is slightly longer in duration than the upstroke (53.5% of a normalized cycle). Wingbeat duration averaged 71.75 ms (S.D. = 7.58, N = 230), which is equivalent to a wingbeat frequency of 13.94 Hz. The two transitional phases are characterized by other distinctive movements that occur as the wings reverse directions, including humeral protraction-retraction (expressed in terms of the angle between the humeral axis and the longitudinal axis of the body); humeral rotation; flexion and extension at the elbow; flexion (= ulnar deviation) and extension (= radial deviation) at the wrist; and abduction (= dorsal deviation) and adduction (ventral deviation) at the wrist.

At the beginning of downstroke, the humerus is protracted about 55°, an orientation that is maintained until the downstroke-upstroke transition, and is elevated 80–90° above horizontal (thus lying in or near a sagittal plane; Fig. 6A). Both elbow and wrist are extended to 90° or slightly less. As downstroke proceeds, the elbow and wrist continue to extend (Fig. 6B), reaching a maxi-

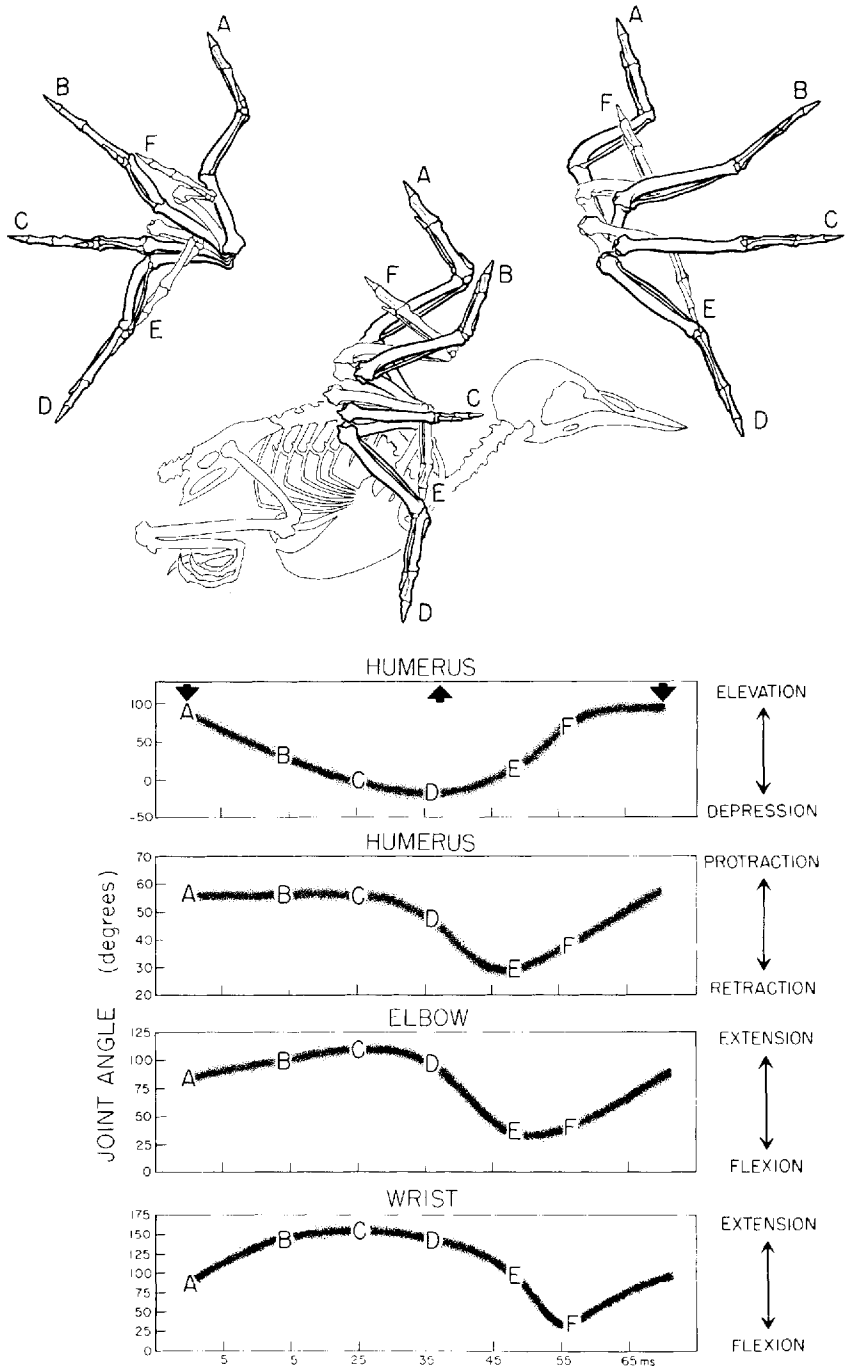

Fig. 6. The movements of the wing in the European starling (*Sturnus vulgaris*). Major phases of the wingbeat cycle are depicted above in lateral view (center), anterolateral view (upper left) and posterolateral view (upper right): A is the beginning of downstroke, B and C depict successive downstroke positions, D represents the downstroke-upstroke transition, and E and F depict two successive upstroke positions. The charts below represent estimated joint angle excursions based on skeletal reconstructions; these reconstructions were mounted to conform with perceived angles recorded from lateral and dorsoventral cineradiographic projections.

mum of 110–120° and 150–160°, respectively, as the humerus passes through a horizontal orientation (Fig. 6C).

During the downstroke-upstroke transition, the humerus depresses 20° below horizontal, completing its downward excursion, and begins to retract (Fig. 6D). The distal wing, in contrast, is depressed well below the level of the humerus through slight humeral rotation, which tips the antebrachium ventrally, and through adduction of the carpometacarpus. Flexion of both elbow and carpometacarpal joints begins.

At the beginning of upstroke, the humerus elevates and continues to be retracted as the elbow and wrist joints are flexing (Fig. 6E). A rapid counterrotation of the humerus during mid-upstroke reorients the ventral surface of the wing to face laterad. Retraction of the humerus (to within about 30° of the body axis) is completed early in upstroke, and thereafter the humerus begins to protract as elevation continues. Extension of the elbow and then extension of the carpometacarpal joint follow sequentially.

During the upstroke-downstroke transition, the humerus reaches its fully elevated position in or near a sagittal plane but continues to protract (Fig. 6F–A). Protraction ceases when angles of about 55° are attained and downstroke is initiated through humeral depression. Extension of the elbow and carpometacarpal joints, which begins in upstroke, continues through the upstroke-downstroke transition into downstroke.

Electromyography

Electromyographic activity in eleven muscles sampled from sixteen birds flying at windspeeds of 9–20 m s^{-1} reveals consistent patterns (Figs. 7,8; Table 1). Downstroke muscles (pectoralis, sternocoracoideus, coracobrachialis caudalis, subscapularis, and humerotriceps) activate during upstroke, and continue their activity through the upstroke-downstroke transition into downstroke (hatched bars, Fig. 8). Upstroke muscles (supracoracoideus, deltoideus major pars cranialis and pars caudalis) activate in the later part of downstroke, continuing into early upstroke (stippled bars, Fig. 8). The remaining three muscles cannot be classified with either group. The scapulohumeralis caudalis and scapulotriceps have activity confined to the downstroke alone, as is one of two bursts of the biceps brachii; the other burst of the biceps brachii is associated with the downstroke group.

All downstroke muscles are activated before downstroke begins (as defined by the initiation of humeral depression). The sternocoracoideus is activated first, followed sequentially by the humerotriceps and then almost immediately by the two parts of the pectoralis. The pars sternobrachialis consistently leads the pars thoracobrachialis (Student's Paired T-Test, $P < 0.001$, $N = 40$) by an average of 4.2 ms, or about 3.4% of a normalized wingbeat cycle. EMGs from both parts of the pectoralis typically exhibit two periods of high amplitude signals coinciding with late upstroke and early downstroke, respectively, and an intermediate period of lower amplitude signals during the upstroke-downstroke transition (Fig. 7A); a similar pattern occurs in pigeons (*Columba livia* [Dial et al., '87, '88]). The coracobrachialis caudalis is the most variable muscle in its duration period, and in comparison to other downstroke muscles exhibits relatively low activity (Fig. 7A). The sternocoracoideus is the first of the downstroke group to cease activity; signal amplitude is greatest prior to the initiation of humeral depression, and rapidly diminishes thereafter (Fig. 7D).

All upstroke muscles are activated in late downstroke, well before upstroke begins (Fig. 8). The scapulotriceps is activated first, followed sequentially by the cranial deltoid, biceps brachii, supracoracoideus, and caudal deltoid. As in the pectoralis, in which the mean duration of activity in upstroke and downstroke is the same, supracoracoideus activity is likewise evenly divided between downstroke and upstroke. Similarly, the supracoracoideus exhibits a diminution in spike amplitude at the downstroke-upstroke transition, but this feature is not as consistent as in the pectoralis. Occasionally the supracoracoideus emits a signal of low amplitude coincident with that of the pectoralis.

The scapulohumeralis caudalis is the only muscle to commence activity in the first half of downstroke (Fig. 8), and thus overlaps with the subscapularis and coracobrachialis (both downstroke muscles) and all of the upstroke muscles. However, like the scapulotriceps, its signals cease prior to upstroke, and thus their activity periods are confined to downstroke alone.

DISCUSSION

Electromechanical delay and relaxation time

In this study we set out to determine the movements of the wing skeleton during flight

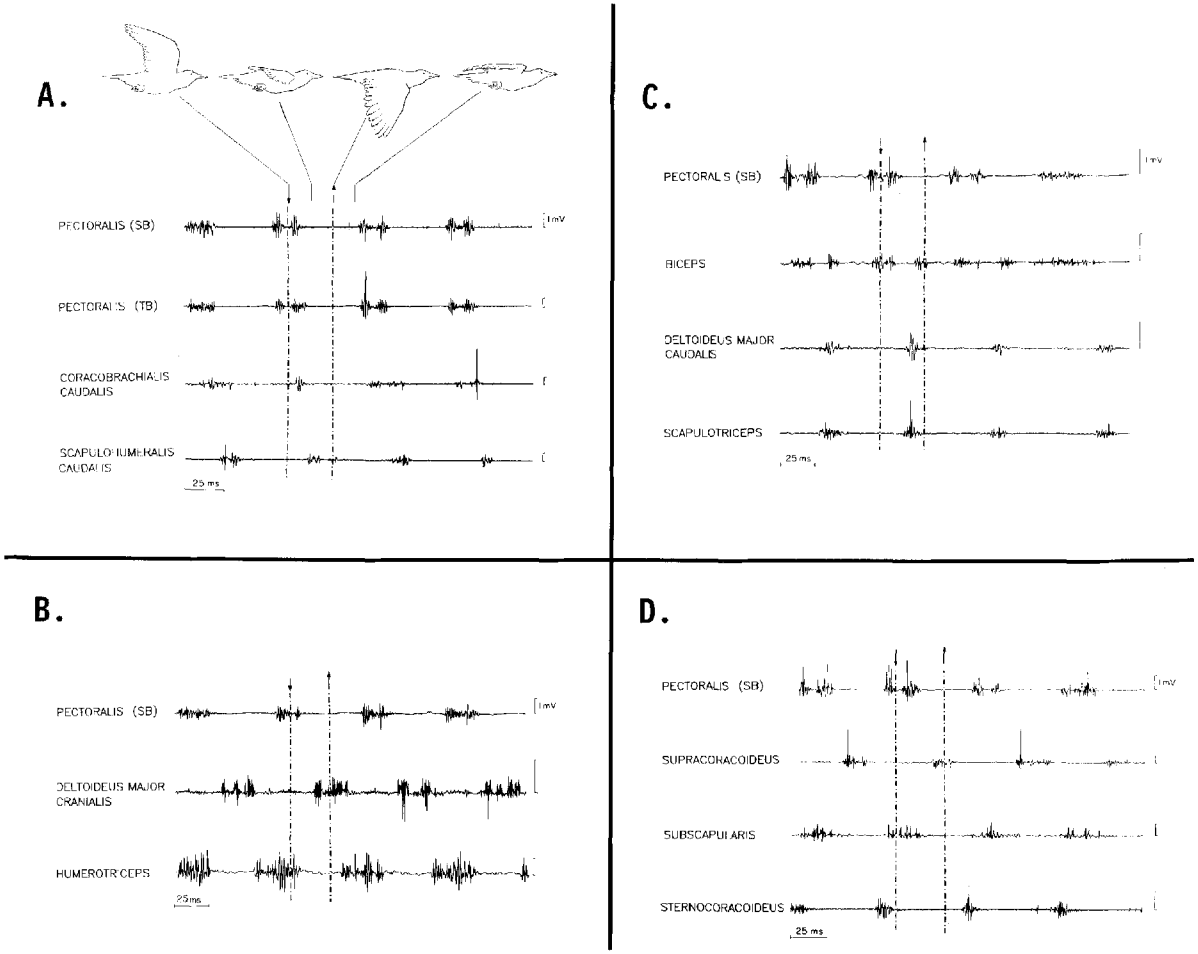

Fig. 7. Representative EMG signals from the shoulder muscles of the European starling (*Sturnus vulgaris*), showing strength (mV) and duration (ms) of signals. Each group of muscles (A–D) was synchronously recorded (with the exception of the humerotriceps, which was recorded from a separate individual and normalized to four wingbeat cycles with the onset of activity from the pectoralis pars sternobrachialis as the reference). A key to the phases of the wingbeat cycle is given by the wing positions illustrated in A. SB, pars sternobrachialis; TB, pars thoracobrachialis.

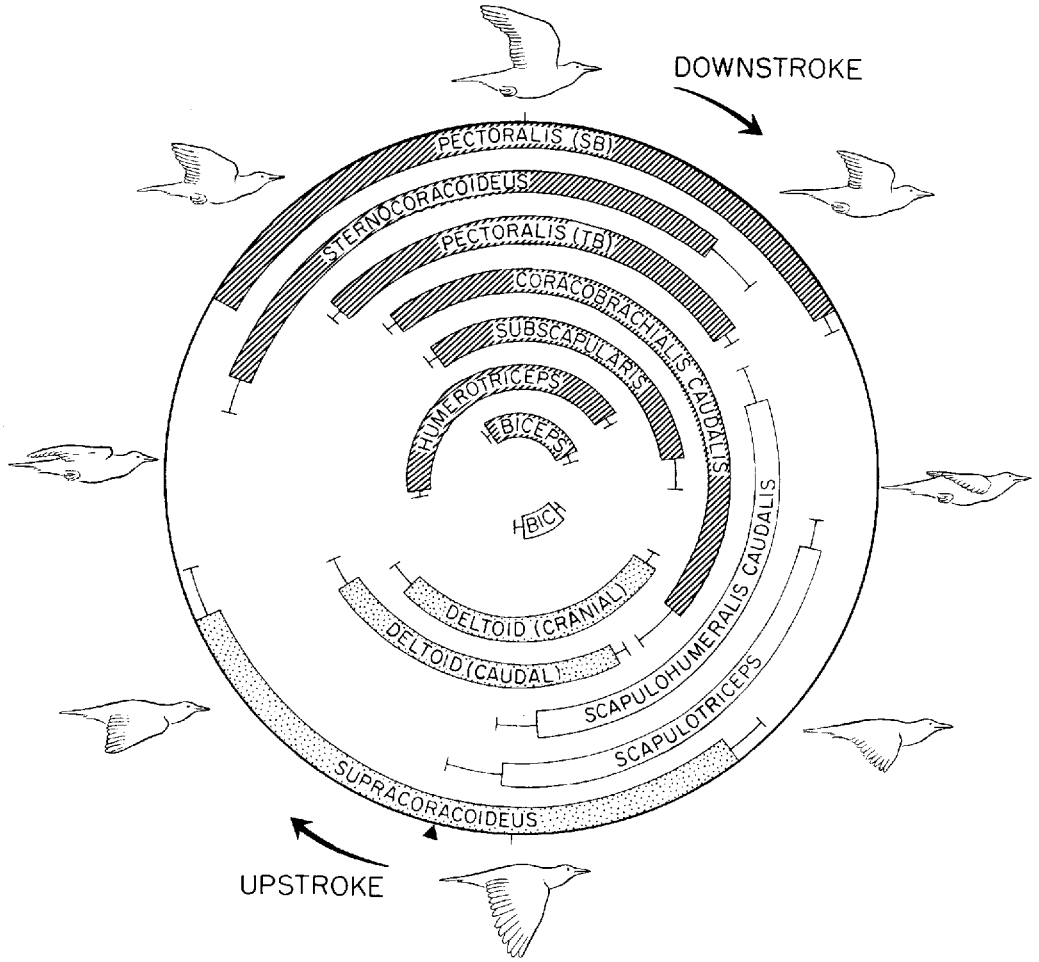

Fig. 8. The cycle of electromyographic activity in the shoulder muscles of the European starling (*Sturnus vulgaris*). For each muscle, mean onset, offset, and Standard Errors (see Table 1) are represented with reference to wing position. Muscles are associated in three groupings: downstroke (hatched), upstroke (stippled), and transitional (unmarked). The black triangle represents the mean initiation of upstroke at 53.5% of a normalized wingbeat cycle. An average wingbeat is 72 ms in duration.

and the electromyographic patterns of muscles associated with these movements. We demonstrate that downstroke muscles are recruited in late upstroke, and that upstroke muscles are recruited in late downstroke. Electromyographic signals from both groups of muscles cease well before the movements that they engender are completed. Although our analysis provides information about the onset and termination of muscle activity and the corresponding movements, we cannot determine the precise contribution of muscles in producing or controlling joint motions. This is a problem universal in kinematic-electromyographic studies that is exacerbated in the present case by the rapidity of wing oscillation. Any attempt to relate EMG activity to specific movements is necessarily constrained by two factors. First, in addition to forces arising from muscle contractions and gravity, forces that produce motion-dependent torques at a joint also influence limb trajectories in a rapidly oscillating system (for a review see Smith and Zernicke, '87). In this study, we have not considered these parameters in any quantitative way. Second, an accurate representation of muscular force requires data on force-velocity

TABLE 1. Statistical summary of the timing of electromyographic signals from the shoulder muscles of European starlings (Sturnus vulgaris)[1]

Muscle	N	Onset(%)	S.E.	Offset(%)	S.E.
Biceps brachii (*first burst*)	20	7.4	1.1	35.0	1.9
Biceps brachii (*second burst*)	20	53.5	1.5	64.5	2.4
Coracobrachialis caudalis	20	6.2	1.0	52.8	3.8
Deltoideus major caudalis	20	59.0	1.6	82.8	2.2
Deltoideus major cranialis	20	51.1	1.5	79.4	2.5
Humerotriceps	20	−10.8	0.5	32.2	1.0
Pectoralis pars sternobrachialis	20	0.0	0.0	33.8	0.9
Pectoralis pars thoracobrachialis	20	3.4	0.7	31.9	0.6
Scapulohumeralis caudalis	20	36.4	2.4	64.7	3.4
Scapulotriceps	20	45.4	1.6	67.5	2.9
Sternocoracoideus	20	−3.1	2.0	27.7	2.9
Subscapularis	10	7.0	1.0	39.7	2.8

[1]In order to compare signals from different birds flying at various windspeeds (9–20 m s^{-1}), the data have been normalized (i.e., as a percentage of the wingbeat cycle, cf. Fig. 8) with the onset of the pectoralis pars sternobrachialis as the zero set point. Downstroke begins at the midpoint of the signal from the pars sternobrachialis, hence 16.9% of a normalized wingbeat cycle from the onset of the signal.

characteristics as well as on the latency (electromechanical delay) that occurs between electrical onset and offset and force development and decay, respectively. In human arm muscles, electromechanical delay varies and is partially dependent on whether the muscle is undergoing a concentric (shortening) or eccentric (lengthening) contraction (Norman and Komi, '79). Latencies of the pectoralis pars sternobrachialis of the European starling were reported by Goslow and Dial ('90), but only for isometric conditions. An electromechanical delay of 3–5 ms was observed from EMG onset to onset of force when stimuli were delivered to the nerve. Isometric twitch times (peak force measured from onset of EMG) were 29–32 ms, and ca. 10 ms from the onset of the EMG to the development of ½ maximum twitch force. One-half relaxation times (times from peak twitch force to one-half peak force during relaxation) were 38–43 ms. At stimulation rates of 100–125 Hz, maximum force was reached in 62–67 ms and force began to decay ca. 22–27 ms after EMG offset. Following EMG offset, total relaxation times were 62–67 ms. Goslow and Dial ('90) recognized, however, that the contractile properties of starling muscle under isometric conditions do not necessarily reflect the force profiles of muscles that are engaged in the rapid oscillation of a wing.

Active stretch-shorten cycling of wing muscles

The sternobrachialis (SB) and thoracobrachialis (TB) parts of the pectoralis and the supracoracoideus begin their electrical activity ca. 15–17 ms before the upstroke-downstroke transition (SB, TB) or downstroke-upstroke transition (supracoracoideus). As a result, each of these muscles apparently undergoes an active stretch-shorten cycle wherein the muscle is first activated as it is being lengthened (during late upstroke for the pectoralis, late downstroke for the supracoracoideus) and subsequently undergoes active shortening. Dial et al. ('87) suggested that this activation pattern in the pectoralis may involve elastic storage during the upstroke and increased force during the downstroke. Biewener et al. ('88) measured *in vivo* forces in the Achilles tendon of jumping kangaroo rats, and found them to be 175% of the maximal isometric forces that may be elicited by stimulating ankle extensors. Their finding underscores the potential importance of active stretch-shorten cycles for locomotion. It is less clear to what degree other muscles of the starling shoulder exhibit a similar stretch-shorten pattern.

Inferences of muscle function

Despite uncertainties introduced by electromechanical delays and relaxation times, certain inferences may be drawn about the functions of individual muscles during the wingbeat cycle.

Downstroke muscle activity begins in late upstroke, and is related to the spreading of the shoulders and the deceleration, extension, and protraction of the wing that occur at the upstroke-downstroke transition. The humerotriceps is activated first, initiating extension of the wing in anticipation of downstroke. Activation of the sternocoracoideus follows, translating the coracoid posterolaterally along the arcuate track of the coracosternal joint. The resulting movement entails a substantial lateral deflection of the acrocoracoid processes to which each dorsal process of

the furcula (Epicleideum) is ligamentously bound. As a result, the shoulders spread and the furcular shafts bend laterad (Jenkins et al., '88).

Following the sternocoracoideus, the pectoralis is activated. As the wing is still elevating during this phase of the wingbeat cycle, the muscle is stretched under active tension and initially must have a decelerative effect on the upstroke. Once the humerus has completely elevated and lies in or near a sagittal plane, the humerus is protracted prior to the major depressive movement of downstroke. Protractive force could be supplied by both the pectoralis and biceps brachii. The larger pars sternobrachialis of the pectoralis consistently leads the pars thoracobrachialis by a few milliseconds, and its cranioventrally directed fibers (particularly those originating from the furcular shafts, which are being bent laterad) are appropriately aligned to effect protraction (Fig. 1). The tendon of the long head of the biceps reaches the acrocoracoid across the craniolateral side of the shoulder joint when the humerus is elevated (Fig. 2); in this position, the biceps may contribute a protractive force.

The biceps brachii, coracobrachialis caudalis, and subscapularis are activated nearly simultaneously in late upstroke after the pectoralis. Although all three of these muscles contribute to humeral depression during downstroke, only the subscapularis would appear to be solely a depressor. The other muscles, as is the case for the pectoralis, may have several functions. The biceps is initially activated when the elbow is extending in late upstroke. Its action at this point can be interpreted only as decelerating elbow extension at the same time as it provides a protractive moment about the shoulder. During the early part of downstroke, the biceps may assist humeral depression; simultaneously, however, it must exert a flexor moment about an extending elbow.

The transition between the activation periods of the downstroke and upstroke muscles is bridged by three muscles. The coracobrachialis caudalis, which is activated longer than any other recorded wing muscle (about 47% of the wingbeat cycle), contributes to humeral depression during early downstroke, after all other depressors are electrically silent. At this point in the wingbeat cycle, humeral depression has been mostly completed, and with the humerus in this position the coracobrachialis caudalis should exert a retractive force. Retraction and ventral rotation of the humerus begin more or less simultaneously near the end of downstroke. Although rotation is completed by the end of downstroke, humeral retraction continues into upstroke. The scapulohumeralis caudalis, a relatively large muscle (Figs. 4, 5) activated midway through downstroke, serves as the primary rotator and retractor of the humerus. The scapulotriceps is then activated. This finding appears to be anomalous, given the fact that the elbow is already fully extended during the second half of downstroke and subsequently begins to flex at the downstroke-upstroke transition. A plausible interpretation is that the activity of this part of the triceps initially controls elbow position in opposition to a flexor torque due to wing loading; the torque is increased by the subsequent activation of the biceps during the end of downstroke. Further increase in the flexor moment may also result from the inertia of the distal wing as the humerus is rapidly retracted in early upstroke. Although the precise nature and magnitude of flexor torques about the elbow remain undetermined at present, the activity pattern of the scapulotriceps is sufficient to infer that these muscles function to stabilize the elbow during the second half of downstroke and into early upstroke. The scapulotriceps may be inferred to have another function as well. The scapulotriceps passes behind the shoulder joint and is thus positioned to assist humeral retraction.

The interpretation of the supracoracoideus and two deltoids, which are activated in late downstroke after the triceps, appears relatively straightforward. Initially, the supracoracoideus must act to decelerate and subsequently to elevate and dorsally rotate the humerus; the latter function is interpreted on the basis of the insertion of the supracoracoideus tendon on the craniodorsal aspect of the proximal humerus (Fig. 3, top). The cranial deltoid appears to be primarily a dorsal rotator by virtue of its broad insertion along the cranial margin of the humerus (Fig. 3); its origin from the Os humerocapsularis provides almost no moment arm for elevating the humerus. The caudal deltoid, in contrast, passes over the shoulder joint and in part wraps around the Os humerocapsularis; its position is consistent with an elevating and retracting action.

Conservatism in tetrapod shoulder muscles

Jenkins and Goslow ('83) compared EMG data from shoulder muscles in the Savannah

Monitor lizard, *Varanus exanthematicus,* and the Virginia opossum, *Didelphis virginiana.* They identified a number of muscles that were "functionally equivalent," that is, similar in attachments, in activity patterns with respect to phases of the locomotor cycle, and in apparent actions. They interpreted these muscles as representing a pattern inherited from the common ancestors of higher tetrapods. One of the purposes of the present study was to generate data from birds that might be compared to those known from other tetrapods, and thus test to what extent conservatism is a general phenomenon.

There are several inherent difficulties in comparing muscle activity patterns among distantly related species. First is the uncertainty over the homology of certain muscles, and the impossibility of making a complete comparison between two species in which the number of shoulder muscles differs (for example, in *Varanus* there are 16 muscles *versus* 15 in *Didelphis*). We can therefore confidently assess only a select few, namely biceps brachii, coracobrachialis, deltoideus, latissimus dorsi, pectoralis, serratus anterior, subscapularis, and triceps. In these cases the similarities in topographic relations and attachments are so great that an assumption of homology is justified in the absence of contrary evidence. Secondly, the framework of our comparison is limited to the two major phases of the locomotor cycle: propulsion (downstroke) *versus* swing (upstroke). Although this level of resolution is relatively gross and does not take into account such details as neuromuscular organization and function, the timing of muscles within the phases of a normalized locomotor cycle is a standard basis on which divergent taxa may be compared.

Electromyographic data from selected shoulder muscles in a lizard (*Varanus exanthematicus*), terrestrial mammals (Virginia opossum, *Didelphis virginiana;* domestic dog, *Canis familiaris*), a bat (*Antrozous pallidus*) and a bird (*Sturnus vulgaris*) reveal three patterns (Fig. 9). First, some muscles are clearly comparable across all of these taxa. The pectoralis is consistently a propulsive-phase muscle that initiates activity in the latter part of swing or upstroke. The subscapularis is similarly patterned (with the exception of a second burst of activity at the downstroke-upstroke transition in *Antrozous;* Hermanson and Altenbach ('83) also reported that low amplitude EMG signals occasionally appear between the two primary bursts). The scapular deltoid is uniformly a swing-phase muscle; its earlier onset in both birds and bats is probably related to the rapidity of wing oscillation.

Data from other muscles that may be comparable are less complete. The activity patterns of the coracobrachialis in *Varanus* and *Sturnus* are very similar, but information is lacking for any mammal. *Varanus, Didelphis,* and *Antrozous* share similarities in the timing of both the latissimus dorsi and serratus anterior, but there are no EMG data from a bird. In *Sturnus,* as in other birds, the latissimus dorsi is reduced to a pair of thin, straplike muscles (latissimus dorsi cranialis et caudalis); the broad, middle part of the muscle as it is typically developed is missing.

A second category of muscles includes those that do not exhibit similar activity patterns across species. The teres major in *Didelphis* is activated at the propulsive-swing transition, whereas in *Antrozous* activity is biphasic with discrete bursts in the propulsive and swing phases. In *Varanus,* the scapulohumeralis caudalis is likewise biphasic, but in *Sturnus* its activity is confined to the downstroke. Data from the sternocoracoideus in *Varanus* and *Sturnus* also provide evidence of functional divergence (no homologue appears to exist in mammals, with the possible exception of monotremes). In *Varanus,* the sternocoracoideus is biphasic; propulsive-phase activity effects sternocoracoid translation, whereas swing-phase activity controls an opposite movement engendered by the elastic sternocoracoid capsule. The sternocoracoideus of *Sturnus* likewise effects sternocoracoid translation, but it acts only during the upstroke-downstroke transition and is not biphasic.

In a third category are muscles that exhibit differences between terrestrial and flying forms. The triceps are undoubtedly homologous among reptiles, birds, and mammals and represent the most unequivocal example of this phenomenon. The scapular and humeral heads of terrestrial forms (*Varanus, Didelphis, Canis*) serve both postural and propulsive functions and are principally related to the propulsive phase. In contrast, the triceps muscles of *Antrozous* are both related to the upstroke, whereas in *Sturnus* the two heads are activated independently in different parts of the wingbeat cycle (scapulotriceps in downstroke, humerotriceps in upstroke). In terrestrial forms the supracoracoideus and its putative mammalian homologues, the infra- and supraspinatus,

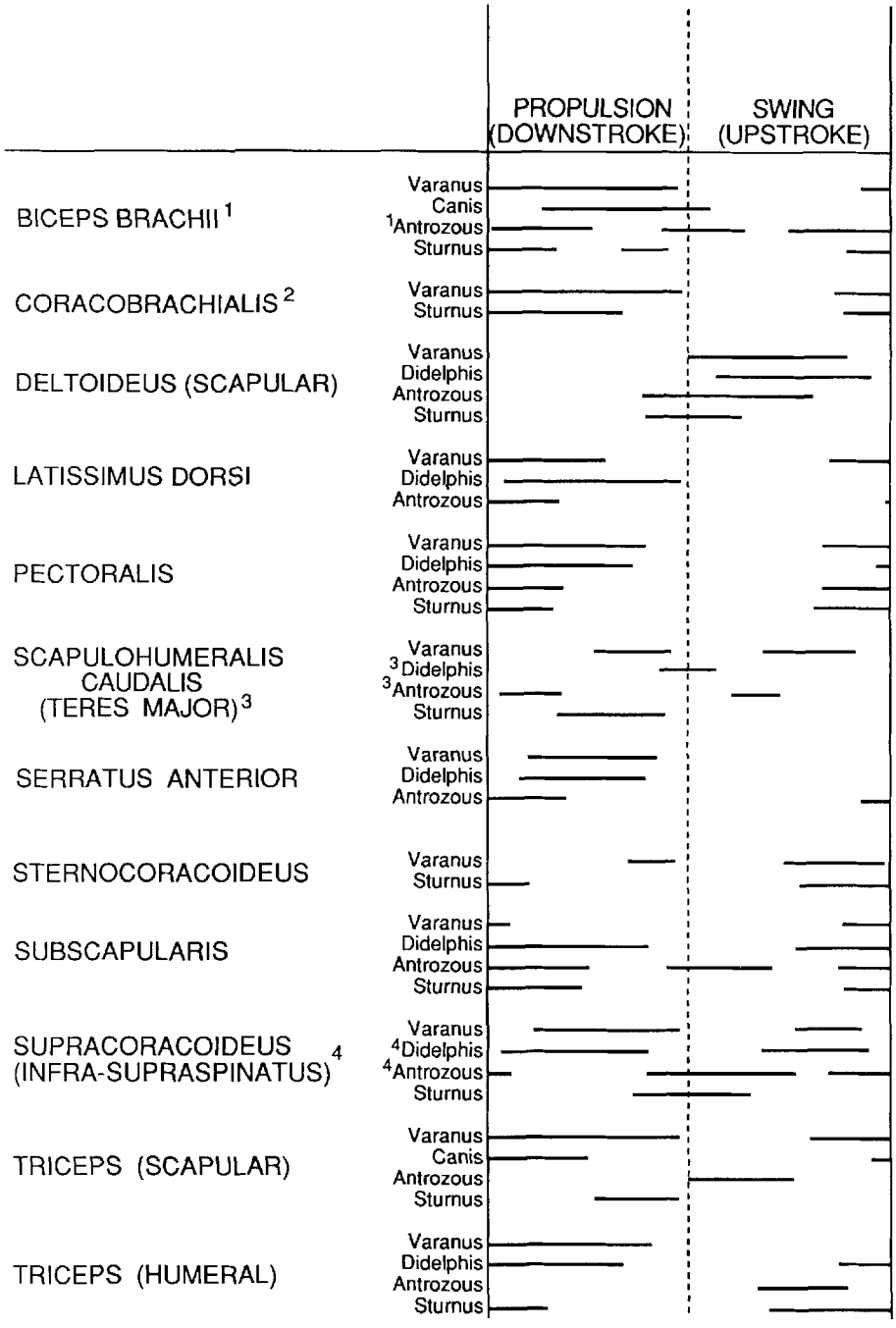

Fig. 9. The electromyographic activity patterns of selected shoulder muscles in the Savannah Monitor lizard (*Varanus exanthematicus* [data from Jenkins and Goslow, '83]), terrestrial mammals (*Canis familiaris* [data from Goslow et al., '81]; *Didelphis virginiana* [data from Jenkins and Weijs, '79]), the Pallid bat (*Antrozous pallidus* [data from Hermanson and Altenbach, '83]) and the European starling (data from this paper). For comparative purposes the data have been normalized to propulsive (= downstroke) and swing (= upstroke) phases of equal duration. Biceps brachii[1] data from *Antrozous* represent the glenoid head; the coracoid head is also biphasic, but the two bursts occur within the downstroke and upstroke phases, respectively. Coracobrachialis[2] data are from the coracobrachialis longus et brevis of *Varanus* and from the coracobrachialis caudalis of *Sturnus*. The homologies of the teres major[3] and infraspinatus+ supraspinatus[4] are putative.

are biphasic, with discrete bursts confined within the propulsive and swing phases. The phasic activity of the homologous muscles in *Antrozous* and *Sturnus* are shifted to the downstroke-upstroke transition, and would appear to be related primarily to the upstroke. A second burst in *Antrozous* lasts through the upstroke-downstroke transition, and comparable activity is also occasionally seen in *Sturnus* at this point. Finally, activity of the biceps brachii in terrestrial forms occurs in conjunction with the propulsive phase only, whereas in fliers the muscle is biphasic, with signals that anticipate both phases.

Some of the differences between terrestrial and flying forms may be related to frequency of limb movement. Recent studies of locomotor and non-locomotor movements in cats have provided evidence that neuromuscular activity patterns may shift under different dynamical regimes (Smith et al., '85; Hoy et al., '85; Smith and Zernicke, '87). During rapid shaking of the paw, the flexors of the knee and ankle are recruited during extension, and the extensors during flexion, to decelerate and reverse joint motions produced under rapidly oscillating torques. These patterns differ from those observed during locomotion and other less rapid movements, and reveal that the relative onset of some muscles (notably the tibialis anterior and vastus lateralis) varies between individuals. The rapid oscillation of the starling's wing (12–16 Hz) may be dynamically analogous to the cat's paw shake (8–12 Hz), and thus may account for the observed shift in pattern of both the scapulotriceps and biceps brachii. Muscles are responsible not only for providing postural and locomotor forces but must also be responsive to the need for controlling torques generated by rapidly moving, segmented limbs (Smith and Zernicke, '87).

From the patterns illustrated in Figure 9 we conclude that three muscles (pectoralis, deltoideus, and subscapularis) may be considered to be conservative with regard to the timing of their participation in the locomotor cycle. This conservatism persists in widely divergent taxa and despite evident differences in the gross anatomical arrangement of the muscles. Other muscles shift their timing, apparently in response to the mechanical demands of different locomotor modes. The triceps is an unequivocal example of such lability. The position and attachments of the triceps heads are compelling evidence of the homology of this group among tetrapods, but the activity patterns differ substantially between terrestrial and flying forms and may even, as in the case of *Sturnus,* differ between individual heads.

ACKNOWLEDGMENTS

We thank H.O. Hooper (Organized Research Committee of Northern Arizona University) for funds to construct the wind tunnel. K. Saczalski and P. Frankiw assisted in the design and construction of the wind tunnel, and J.D. Harry, R.A. Meyers, and D.S. Wilson assisted with various experiments. We acknowledge A.S. Parsa (Siemens Corporation) for his astute technical support in maintaining the cineradiographic equipment. L. Laszlo Meszoly prepared the figures. This study was supported with funds from N.S.F. grants BSR 85-11867 and BSR 87-06820.

LITERATURE CITED

Aulie, A. (1970) Electrical activity from the pectoral muscle of a flying bird, the budgerigar. Comp. Biochem. Physiol. *36:*297–300.

Bemis, W.E., and G.V. Lauder (1986) Morphology and function of the feeding apparatus of the lungfish, *Lepidosiren paradoxa* (Dipnoi). J. Morphol. *187:*81–108.

Biewener, A.A., R. Blickhan, A.K. Perry, N.C. Heglund, and C.R. Taylor (1988) Muscle forces during locomotion in kangaroo rats: Force platform and tendon buckle measurements compared. J. Exp. Biol. *137:*191–205.

Brown, R.H.J. (1948) The flight of birds. I. The flapping cycle of the pigeon. J. Exp. Biol. *25:*322–333.

Brown, R.H.J. (1963) The flight of birds. Biol. Rev. *38:* 460–489.

Dial, K.P., S.R. Kaplan, G.E. Goslow, Jr., and F.A. Jenkins, Jr. (1987) Structure and neural control of the pectoralis in pigeons: Implications for flight mechanics. Anat. Rec. *218:*284–287.

Dial, K.P., S.R. Kaplan, G.E. Goslow, Jr., and F.A. Jenkins, Jr. (1988) A functional analysis of the primary upstroke and downstroke muscles in the domestic pigeon (*Columba livia*) during flight. J. Exp. Biol. *134:*1–16.

Goldspink, G., C. Mills, and K. Schmidt-Nielsen (1978) Electrical activity of the pectoral muscles during gliding and flapping flight in the herring gull (*Larus argentatus*). Experientia *34:*862–865.

Goslow, G.E., Jr., H.J. Seeherman, C.R. Taylor, M.N. McCutchin, and N.C. Heglund (1981) Electrical activity and relative length changes of dog limb muscles as a function of speed and gait. J. Exp. Biol. *94:*15–42.

Goslow, G.E., Jr., and K.P. Dial (1990) Active stretch-shorten contractions of the m. pectoralis in the European starling (*Sturnus vulgaris*): Evidence from electromyography and contractile properties. Neth. J. Zool. *40:*106–114.

Hagiwara, S., S. Chichibu, and N. Simpson (1968) Neuromuscular mechanisms of wing beat in hummingbirds. Z. Vergl. Physiol. *60:*209–218.

Hermanson, J.W., and J.S. Altenbach (1983) The functional anatomy of the shoulder of the Pallid bat, *Antrozous pallidus.* J. Mamm. *64:*62–75.

Hoy, M.G., R.F. Zernicke, and J.L. Smith (1985) Contrasting roles of inertial and muscle moments at knee and

ankle during paw-shake response. J. Neurophysiol. *54:*1282–1294.

Jenkins, F.A., Jr., and G.E. Goslow, Jr. (1983) The functional anatomy of the shoulder of the Savannah Monitor lizard (*Varanus exanthematicus*). J. Morphol. *175:* 195–216.

Jenkins, F.A., Jr., and W.A. Weijs (1979) The functional anatomy of the shoulder in the Virginia opossum (*Didelphis virginiana*). J. Zool., Lond. *188:*379–410.

Jenkins, F.A., Jr., K.P. Dial, and G.E. Goslow, Jr. (1988) A cineradiographic analysis of bird flight: The wishbone in starlings is a spring. Science *241:*1495–1498.

Norman, R.W., and P.V. Komi (1979) Electromechanical delay in skeletal muscle under normal movement conditions. Acta Physiol. Scand. *106:*241–248.

Rayner, J.M.V. (1979a) A new approach to animal flight mechanics. J. Exp. Biol. *80:*17–54.

Rayner, J.M.V. (1979b) A vortex theory of animal flight. Part 2. The forward flight of birds. J. Fluid Mech. *91:*731–763.

Shaffer, H.B., and G.V. Lauder (1985) Aquatic prey capture in ambystomatid salamanders: Patterns of variation in muscle activity. J. Morphol. *183:*273–284.

Simpson, S.F. (1983) The flight mechanism of the pigeon *Columba livia* during take-off. J. Zool., Lond. *200:*435–443.

Smith, J.L., B. Betts, V.R. Edgerton, and R.F. Zernicke (1985) Rapid ankle extension during paw shakes. Selective recruitment of fast ankle extensors. J. Neurophysiol. *43:*612–620.

Smith, J.L., and R.F. Zernicke (1987) Predictions for neural control based on limb dynamics. Trends Neurosci. *10:*123–128.

Torre-Bueno, J.R., and J. Larochelle (1978) The metabolic cost of flight in unrestrained birds. J. Exp. Biol. *75:*223–229.

Vanden Berge, J.C. (1979) Myologia. In J.J. Baumel, A.S. King, A.M. Lucas, J.E. Breazile, and H.E. Evans (eds): Nomina Anatomica Avium. London: Academic Press, pp. 175–219.